

Design, Simulation and Evaluation of Uniform Magnetic Field Systems for Head-Free Eye Movement Recordings with Scleral Search Coils

Karin Eibenberger^{1,2}, Bernhard Eibenberger¹ and Michele Rucci¹

Abstract—The precise measurement of eye movements is important for investigating vision, oculomotor control and vestibular function. The magnetic scleral search coil technique is one of the most precise measurement techniques for recording eye movements with very high spatial (≈ 1 arcmin) and temporal ($> \text{kHz}$) resolution. The technique is based on measuring voltage induced in a search coil through a large magnetic field. This search coil is embedded in a contact lens worn by a human subject. The measured voltage is in direct relationship to the orientation of the eye in space. This requires a magnetic field with a high homogeneity in the center, since otherwise the field inhomogeneity would give the false impression of a rotation of the eye due to a translational movement of the head. To circumvent this problem, a bite bar typically restricts head movement to a minimum. However, the need often emerges to precisely record eye movements under natural viewing conditions. To this end, one needs a uniform magnetic field that is uniform over a large area. In this paper, we present the numerical and finite element simulations of the magnetic flux density of different coil geometries that could be used for search coil recordings. Based on the results, we built a $2.2 \times 2.2 \times 2.2$ meter coil frame with a set of 3×4 coils to generate a 3D magnetic field and compared the measured flux density with our simulation results. In agreement with simulation results, the system yields a highly uniform field enabling high-resolution recordings of eye movements.

I. INTRODUCTION

A. Eye Tracking Using a Magnetic Scleral Search Coil

Originating in the 1960s [9], [2], the search coil technique is still one of the most precise eye movement measurement techniques [7]. The case for the need to precisely record eye movements without restricting head movements has long been made [14]. In recent years, this need has been reinforced by the findings that small fixational eye movements—the eye movements humans continually perform, even when fixating on a single point—are far more controlled than previously thought [4], [8], [12] and appear to serve specific computational functions [5], [11], [13]. A search coil system typically consists of a cubic magnetic field coil system with diameters between 1 and 2.5 meters. The magnetic field system produces two or three oscillating or revolving magnetic fields which are arranged in space quadrature. The orientation of the eye is derived from the voltage induced in small search coils attached to the eyes through a contact lens. The voltages caused by the components of the different

magnetic fields are demodulated and used to calculate eye orientation.

B. Head-Free Eye Tracking

The magnetic field of a cubic search coil system is only homogenous in a very small region in the center of the field system. When deriving eye orientation from induced voltages measured with a search coil, one has to assume that no translational motion of the head had happened, otherwise the inhomogeneity of the magnetic field system will cause a translational movement of the head to be interpreted as rotational movement of the eye. Typically, movements of the subject are therefore restricted by using head holders and bite bars. We, in contrast, want to record eye movements under natural viewing conditions, i.e. with the head free. For this, we need a uniform magnetic field over a large area. Solutions to correct the inhomogeneity of the magnetic field offline exist [15], as well as suggestions of how to improve the magnetic field of a Helmholtz coil [1], [3]. However, this still restricts eye movement recordings to the use of a bite bar and head holder. The only way to allow eye movement recordings with high spatial resolution under natural viewing condition is to use a uniform magnetic field.

II. METHODS

We compare the finite element simulations of four different magnetic field geometries with numerical solutions computed in Matlab. We used the Biot-Savart law to get an approximation of the magnetic field using Matlab (Mathworks, Natick, MA). COMSOL (COMSOL Multiphysics, Stockholm, Sweden) was used for the finite element simulation of the magnetic field system, enabling a more detailed investigation of the whole geometry and the effects of the exact wires and dimensions we used. COMSOL also uses the Biot-Savart law to compute the magnetic field in the AC/DC magnetics toolbox. Based on the results of the simulation, we constructed a $2.2 \times 2.2 \times 2.2$ meter coil frame and measured the magnetic flux density using a coil and compare the simulation results with the measured magnetic field.

A. Coil Geometries

We analyzed the magnetic field of four different coil geometries: the *circular Helmholtz* coil (figure 1A) is usually a reference for the creation of a uniform magnetic field, although not feasible for search coil measurements due to its shape. The most commonly used frame geometry is a modification of a *true square Helmholtz* coil - a *simple square Helmholtz* coil (figure 1B). The difference lies in the

¹College of Arts and Sciences, Department of Psychology, Active Perception Laboratory, Boston University, Boston, MA 02215, USA karineib@bu.edu

²Technical University of Vienna, School of Mechanical and Industrial Engineering, Vienna, Austria

distance between the square coils, which would be $d/2$ (with d being the diameter of the square coil) for a true square Helmholtz coil, but typically the distance equals the diameter for practical purposes. Of the various coil designs that have been extensively discussed in the literature, two additional ones have been picked for comparison. The *Rubens* geometry (figure 1C) [10] has been used in one coil system, and literature search indicated that the 4-coil *Merritt* system (figure 1D) might be most promising for the construction of coil frame with large region of homogeneity [6]. Table I compares the different coil geometries analyzed in this paper.

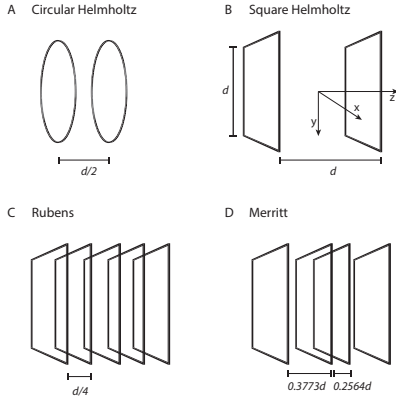


Fig. 1. Configuration of coil designs used to generate uniform magnetic fields. Coil properties are shown in table I.

TABLE I
DIFFERENT COIL GEOMETRIES AND THEIR PROPERTIES

Coil Design	Coil Shape	No. of Coils	Coil Spacing	Ampere-turn Ratio
Circular Helmholtz	circular	2	-0.25d, +0.25d	1/1
Square Helmholtz	square	2	-0.5d, +0.5d	1/1
Rubens	square	5	-0.5d, -0.25d, 0, +0.25d, +0.5d	19/4/10/4/19
Merritt	square	4	-0.5055d, -0.1281d, +0.1281d, +0.5055d	26/11/11/26

B. Numerical Simulation in Matlab

For the analytical simulation in Matlab, we used the Biot-Savart law to describe the magnetic field \vec{B} at position \vec{r} generated by an electric steady current I . The magnetic field of a coil $B(\vec{r})$ can be calculated as the sum

$$B(\vec{r}) = \frac{\mu_0}{4\pi} \sum \frac{I_N \Delta \vec{l} \times \vec{r}}{|\vec{r}|^3} \quad (1)$$

with $I_N = N * I$ being the current in the field coils and N the number of wire turns for each coil, $\Delta \vec{l}$ the wire element, \vec{r} the position vector, $\vec{r} = \vec{r} - \vec{l}$ the displacement vector of each wire element, and μ_0 being the magnetic permeability of vacuum, which equals $4\pi * 10^{-7} \text{ Vs/Am}$.

C. Finite Element Simulation in COMSOL

Comsol Multiphysics was used to simulate the magnetic field of the four different coil systems. The $2.2 \times 2.2 \times 2.2$ meter geometry of the coils was modeled and meshed in 3D in a 1:1 scale using SolidWorks (SolidWorks, Dassault Systèmes SolidWorks Corp, Vélizy-Villacoublay, France) (see figure 2).

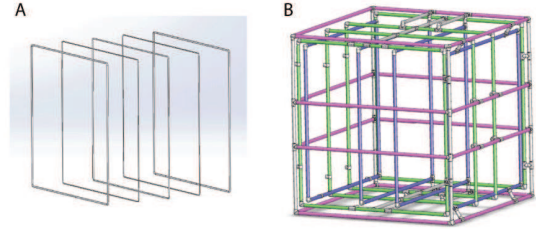


Fig. 2. Example of a coil drawing in SolidWorks. A drawing of one set of coils for the simulation in COMSOL. B A complete 3D Merritt coil system with 3 x 4 coils.

In Comsol Multiphysics, the *AC/DC mf* ('magnetic field') toolbox was used to simulate multi-turn coils with AWG12 wire (American Wire Gauge, Brown&Sharpe), which we also used to construct the coil later on. The coils have a closed geometry with a circular cross section and each wire is insulated. Around the coils, we created a sphere of air with a diameter of 6 meters and an infinite sphere around the air sphere with 1 meter thickness (see figure 3). The direction of current flow was specified by manually selecting a cross-sectional area of each coil, using the numeric coil type. We used 1 A input current for the coils, which are connected in series. As formulated by Ampère's law, a current I in a wire produces a magnetic field \vec{B}

$$\oint \vec{B} d\vec{s} = \mu_0 I \quad (2)$$

and

$$\oint \vec{H} d\vec{s} = I \quad (3)$$

For the distances between the coils and the number of turns used for each coil geometry, see table I. For the Merritt coil, for example, we used 26-11-11-26 turns, respectively. For the circular and square Helmholtz coils that have a 1:1 amperes-to-turn ratio we simulated 10 turns in each coil. We meshed air, infinity space and coils with an adaptive, very fine, user-controlled mesh (see figure 3A).

D. Coil Frame Construction

Based on the results of the simulated homogeneity, we built a Merritt coil frame system (figure 4) consisting of a set of 3 x 4 coils. We used PVC tubes and wood for mechanical support. The inside of the frame can be accessed by lifting the middle horizontal coils with a pulley system. The outer dimensions of the largest set of coils are 2200 x 2200 x 2224 mm. The middle and inner sets of coils have to be

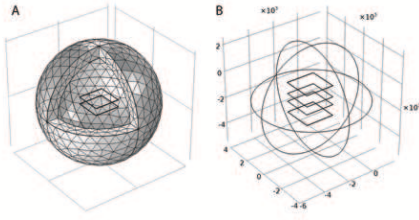


Fig. 3. A Air and infinity sphere with a Helmholtz coil system of two square coils inside. B Merritt 4 coil frame in the COMSOL simulation.



Fig. 4. Merritt 3D coil frame with 3x4 coils. The wires are embedded in the plastic tubing, the wooden frame is for mechanical support. In the center of the frame, a reference coil is mounted which measures the induced voltage as a reference.

slightly smaller in dimension for constructional purposes and are 2080 x 2080 x 2103 mm and 1962 x 1962 x 1984 mm, respectively. The construction is based on the SolidWorks drawing in figure 2.

E. Magnetic Field Measurements

We used a hand-made coil with the diameter of $d = 80\text{mm}$ and $N = 10$ turns to measure the flux density of our coil frame. A signal generator (Tektronix, AFG320) provided the reference value for a PT1-type controller which uses a reference coil mounted inside the frame (it can be seen on the photograph in figure 4) to measure the induced reference (i.e. *actual*) voltage. The magnetic field coil was powered by an audio amplifier (Podium, Pro Audio VX2000) with a self-made resonant driving circuitry. We placed a wooden bar in the center of the magnetic field frame, and placed the coil on 35 defined positions orthogonal to the field, where we measured the induced voltage five times for 100 sweeps at each position with an oscilloscope (LeCroy Waverunner LT322). We calculated mean, median and standard deviation of the measured points. To calculate the magnetic flux density $B(\vec{r})$ by using the measured voltage, we used the relationship

$$U(r) = NB(\vec{r})A\omega \quad (4)$$

with N being the number of turns of the measurement

coil, A being the area of this coil and ω being the frequency of our AC magnetic field, which was driven with 16 kHz.

III. RESULTS

A. Numerical and Finite Element Simulations

Figure 5 shows the 3D visualization of the magnetic field generated by a set of four coils, as simulated using COMSOL.

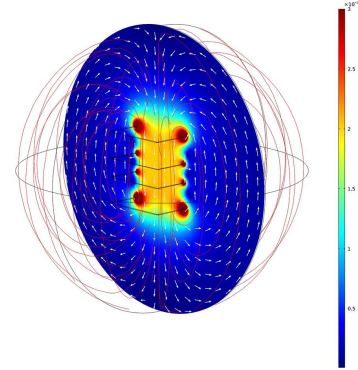


Fig. 5. The magnetic field lines simulated and visualized in COMSOL.

Finite element simulations and numerical simulations deliver highly corresponding results. Figure 6 shows the magnetic field \vec{B} of the four different, simulated coil geometries. The Merritt four coil system delivers the highest magnetic flux density \vec{B} , but a closer look also reveals that it is more homogenous over a larger area compared to the Rubens coil geometry (see figure 7). The graph shows the magnification of the magnetic field in the center of the frame along the z-axis, from -400 to +400 mm, measured from the center. In this region, the inhomogeneity of the Rubens frame geometry ranges from -0.04336% off center to 0.0% in the center of the frame. Compared to this, the Merritt frame has an inhomogeneity ranging from -0.00236% at 400 mm off center to 0.00220%.

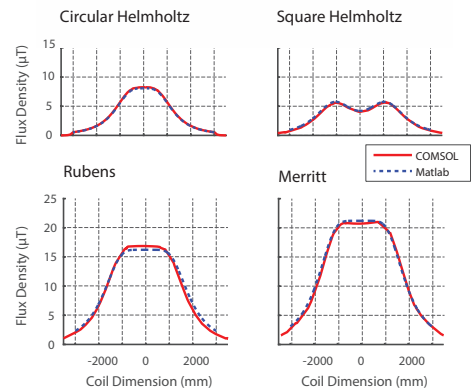


Fig. 6. Simulation of the magnetic field along the z-axis of the coil frame of four different coil geometries.

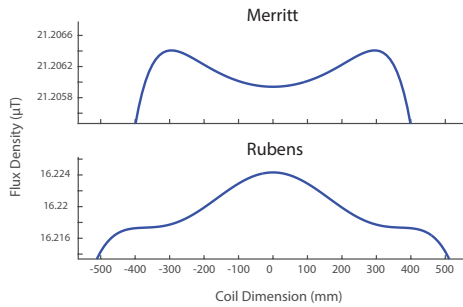


Fig. 7. Simulation of the magnetic field along the z-axis of the coil frame of the Rubens and Merritt coil geometry, magnified. Note that here, the scaling of the y-axis is different by the order of 10.

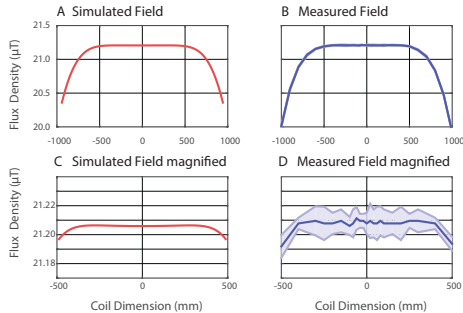


Fig. 8. Comparison of magnetic field along the z-axis of the coil frame of the simulation of the Merritt coil geometry versus measured magnetic field along the z-axis of the realized geometry of the system shown on figure 4. The measured magnetic field is given as mean, the shaded area represents \pm standard deviation. The upper graphs show the magnetic field along the whole two meters of the frame. The graphs below show the magnetic field in the center of the frame.

B. Field Measurement

The resulting magnetic field of the realized frame system comes very close to the simulation in homogeneity and field strength. We measured pre-defined points along the z-axis of the field five times and show the mean and standard deviation of the measured magnetic field in figure 8. The error of the measurement in the range of ± 400 mm is below 0.05% which is within the accuracy of the oscilloscope we used.

IV. CONCLUSION

Since we want to record eye movements without constraining head motion to a very limited region in the very center of the magnetic coil frame, we needed a coil geometry that produces a homogenous field over a large area. Regular search coil systems use only a square Helmholtz coil configuration, and subject are typically seated in the center of the frame while any head motion is prevented by using a bite bar. However, for a head-free recording, the regular Helmholtz geometry is not suitable and the magnetic field is in fact very inhomogeneous. Different coil systems for a magnetic field with a larger homogeneous area have been extensively discussed in the literature, but only one - the Rubens coil geometry - was used as a the base for a search coil system. The Rubens geometry does deliver a quite homogeneous magnetic field, however, the geometry was proposed in 1945 and other coil geometries have been proposed since then,

one of them being the Merritt geometry. We simulated the magnetic flux density numerically and with finite elements using the actual physical properties of the wires and the multi-turn coils. We concluded that the Merritt geometry is better in terms of uniform magnetic flux density, having less error in the uniformity by an order of approximately 20 compared to the Rubens frame geometry. Based on the simulation results, we constructed a field coil system of $2.2 \times 2.2 \times 2.2$ meter size and measured the voltage induced in a coil along the center line of one field to calculate the magnetic field of our frame. The resulting field is highly homogenous over a wide area, enabling head-free search coil measurements in a spherical area of about 1 meter.

ACKNOWLEDGMENT

This work was supported by National Science Foundation grant BCS-1457238 and National Institutes of Health grant EY18363.

REFERENCES

- [1] Vernon Barger and Martin G Olsson. *Classical electricity and magnetism: a contemporary perspective*. Allyn & Bacon, 1987.
- [2] H. Collewijn, F. van der Mark, and T. C. Jansen. Precise recording of human eye movements. 15(3):447–450, 1975.
- [3] Jochen Ditterich and Thomas Eggert. Improving the homogeneity of the magnetic field in the magnetic search coil technique. *Biomedical Engineering, IEEE Transactions on*, 48(10):1178–1185, 2001.
- [4] Hee-kyoung Ko, Martina Poletti, and Michele Rucci. Microsaccades precisely relocate gaze in a high visual acuity task. *Nature neuroscience*, 13(12):1549–1553, 2010.
- [5] Xutao Kuang, Martina Poletti, Jonathan D Victor, and Michele Rucci. Temporal encoding of spatial information during active visual fixation. *Current Biology*, 22(6):510–514, 2012.
- [6] R Merritt, C Purcell, and G Stroink. Uniform magnetic field produced by three, four, and five square coils. *Review of Scientific Instruments*, 54(7):879–882, 1983.
- [7] Jorge Otero-Millan, Dale C Roberts, Adrian Lasker, David S Zee, and Amir Kheradmand. Knowing what the brain is seeing in three dimensions: A novel, noninvasive, sensitive, accurate, and low-noise technique for measuring ocular torsion. *Journal of vision*, 15(14):11–11, 2015.
- [8] Martina Poletti, Murat Aytekin, and Michele Rucci. Head-eye coordination at a microscopic scale. *Current Biology*, 25(24):3253–3259, 2015.
- [9] D. A. Robinson. A method of measuring eye movement using scleral search coil in a magnetic field. *IEEE Trans Biomed Eng*, 10:137–145, Oct 1963.
- [10] Sidney M. Rubens. Cube-surface coil for producing a uniform magnetic field. *Review of Scientific Instruments*, 16(9):243–245, 1945.
- [11] Michele Rucci and Antonino Casile. Decorrelation of neural activity during fixational instability: Possible implications for the refinement of v1 receptive fields. *Visual neuroscience*, 21(05):725–738, 2004.
- [12] Michele Rucci and Martina Poletti. Control and functions of fixational eye movements. *Annual Review of Vision Science*, 1:499–518, 2015.
- [13] Michele Rucci, Martina Poletti, Jonathan Victor, and Marco Boi. Contributions of eye movement transients to spatial vision. *Journal of vision*, 15(12):211–211, 2015.
- [14] Robert M Steinman, Eileen Kowler, and Han Collewijn. New directions for oculomotor research. *Vision research*, 30(11):1845–1864, 1990.
- [15] Jakob S Thomassen, Giacomo Di Benedetto, and Bernhard JM Hess. Decoding 3d search coil signals in a non-homogeneous magnetic field. *Vision research*, 50(13):1203–1213, 2010.